Astronomy & Astrophysics manuscript no. AA˙2003˙0494 February 2, 2008
(DOI: will be inserted by hand later)

Properties of RR Lyrae stars in the Inner Regions of the Large Magellanic Cloud. ⋆

J. Borissova[1], D. Minniti[1], M. Rejkuba[2], D. Alves[3], K. H. Cook[4], and K. C. Freeman[5].

[1] Department of Astronomy, P. Universidad Católica, Av. Vicuña Mackenna 4860, Casilla 306, Santiago 22, Chile
e-mail: jborisso, dante@astro.puc.cl
[2] European Southern Observatory, Karl-Schwarzschild-Str. 2, D-85748 Garching b. München, Germany
e-mail: mrejkuba@eso.org
[3] Columbia University, Dept. of Astronomy, New York, USA
e-mail: alves@astro.columbia.edu
[4] Lawrence Livermore National Laboratory, Livermore, California, USA
e-mail: kcook@llnl.org
[5] Mount Stromlo Observatory, Canberra ACT, Australia
e-mail: kcf@mso.anu.edu

Received .. ... 2003; accepted 2003

Abstract. We present the radial velocities, metallicities and the K-band magnitudes of 74 RR Lyrae stars in the inner regions of the LMC. The intermediate resolution spectra and infrared images were obtained with FORS1 at the ESO VLT and with the SOFI infrared imager at the ESO NTT. The best 43 RR Lyrae with measured velocities yield an observed velocity dispersion of $\sigma = 61 \pm 7$ km s^{-1}. We obtain a true LMC RR Lyrae velocity dispersion of $\sigma = 53$ km s^{-1}, which is higher than the velocity dispersion of any other LMC population previously measured. This is the first empirical evidence for a kinematically hot, metal-poor halo in the LMC as discussed in Minniti et al. (2003). Using Layden's (1994) modification of the ΔS method we measured the metallicity for 23 of our stars. The mean value is [Fe/H] $=-1.46 \pm 0.09$ dex. The absolute magnitudes M_V and M_K of RR Lyrae stars are linear functions of metallicity. In the V band, our data agree with the Olech et al. (2003) relation, in the K band the slope is flatter. The average apparent V luminosity of 70 RR Lyrae stars is $< V >= 19.45 \pm 0.04$ and the average K luminosity of 37 RR Lyrae stars is $< K >= 18.20 \pm 0.06$. There is no obvious relation between apparent V magnitude and LogP, while the RR Lyrae K band magnitudes show a well defined linear trend with LogP. Using the Bono et al. (2001) and Bono et al. (2003) theoretical Near-Infrared Period-Luminosity-Metallicity relations we calculate the LMC distance modulus $\mu_0 = 18.48 \pm 0.08$.

Key words. :Galaxies: individual (LMC) – Galaxies: Formation – Stars: RR Lyrae

1. Introduction

RR Lyrae stars are old ($t \gtrsim 10^{10}$ yr), metal-poor ($-2.5 <$ [Fe/H] < -0.5) pulsating variables. They are one of the most important steps in the distance ladder, and are also one of the best tracers of the primordial populations of the Milky Way. Their characteristic light curves make them easy to find in large microlensing surveys like the MACHO Project.

Studies of the LMC kinematics (Alves & Nelson 2000, Graff et al. 2000, Gyuk et al. 2000, Hardy et al. 2001, van der Marel et al. 2002) suggest that if they lie in a disk, like the globular clusters, the RR Lyrae stars would show fairly rapid systemic rotation (about ± 40 km s^{-1}), and a velocity dispersion of about $15-30$ km s^{-1}. If they belong to a metal-poor halo, then the rotation will be low and the velocity dispersion will be about 50 km s^{-1}.

Walker (1992) measured the abundances of 182 RR Lyrae stars from the period-amplitude relation in seven LMC clusters (NGC 2257, Reticulum, NGC 1841, NGC 1466, NGC 1766, NGC 2210, NGC 1835). They fall in the interval -1.7 to -2.3, with the mean value [Fe/H]$=-1.9 \pm 0.2$ dex. Recently, Clementini et al. (2003) measured metallicities of 101 LMC field, RR Lyrae stars using low-resolution spectra obtained with the Very Large

Send offprint requests to: J. Borissova

⋆ Based on observations collected with the Very Large Telescope and the New Technology Telescope of the European Southern Observatory within the Observing Programs 64.N-0176(B) and 70.B-0547. Tables 3, 4 and 6 are also available in electronic form at the CDS via anonymous ftp to cdsarc.u-strasbg.fr (130.79.128.5) or via http://cdsweb.u-strasbg.fr/cgi-bin/qcat?J/A+A/

Telescope. They found metallicities between -0.5 and -2.1, with an average value of [Fe/H]=-1.46 ± 0.3 dex.

The distance to the LMC has been the subject of many studies. There is a well known discrepancy of 0.2—0.3 mag between distances derived from Population I and II indicators. Population I distance indicators give a long distance modulus for the LMC, in the range from 18.5 to 18.7 mag, while Population II indicators support a shorter modulus in the range from 18.4 to 18.6. Clementini et al. (2003) summarized most of the distance determinations and using accurate photometry of 101 RR Lyrae stars, reported a common value of $\mu = 18.515 \pm 0.085$ mag.

The goal of this project is to measure the properties (kinematics, distributions, abundances and distances) of the RR Lyrae stars in six selected inner region fields of the LMC. To use the LMC RR Lyrae as tracers of a putative LMC halo is not a new idea. Kinman et al. (1991), and Feast (1992) review the problem of measuring their kinematics. Because these LMC RR Lyrae stars are faint ($19 < V < 20$), ten years ago this project was beyond the reach of the best telescopes. Metallicities and distance determination are additional products of this project.

2. Observations and Reductions

2.1. Selection of the sample

We have chosen our sample of RR Lyrae stars using the MACHO database from six central fields of the LMC bar, at distances from 0.7 to 1.5 degrees away from the rotation center. As a control sample for the LMC kinematic properties, we also selected known long period variables (LPV) from MACHO and OGLE (Zebrun et al. 2001) and Cepheids from the MACHO catalog in the same fields. The observed fields are shown on Fig. 1 and are summarized in Table 1. The fields are centered on the source stars of the LMC microlensing events discovered by MACHO Project (Alcock et al. 2001). The number of stars for each field with spectra and/or K band magnitudes is also given in the last column.

Fig. 1. This is MACHO image (http://www.macho.mcmaster. ca/) of LMC (R-band) showing the location of the MACHO fields and the fields for which we obtained MOS spectra and K band photometry. North is up and east is to the left. The small thick boxes indicate the $7' \times 7'$ field of view of the CCD images.

The distribution over the period of our RR Lyrae stars is shown on Fig. 2. The solid line represents RRab stars, while the dotted line marks RRc+RRe stars. Our sample of RRab stars covers the interval from 0.35 days to the 0.75 days (only one star has period of 0.97 days), with a mean value of 0.572 ± 0.09 days, the RRc stars range from 0.25 to 0.43 days and the mean period is 0.352 ± 0.05 days. The mean periods of our RRab Lyrae sample is in good agreement with values determined by the MACHO team from approx. 7900 RR Lyrae stars: $\langle P_{ab} \rangle = 0.583$ days (Alcock et al. 1996) and the recent work of the OGLE team (Soszynski et al. 2003): $\langle P_{ab} \rangle = 0.573$ days. For RRc stars the mean periods are $\langle P_c \rangle = 0.342$ days, from the MACHO team, and $\langle P_c \rangle = 0.339$, from the OGLE team. Therefore, despite the limited sample number, the properties of RR Lyrae stars in our sample should be representative of the whole population.

Soszynski et al. (2003) present the period distribution for OGLE RR Lyrae in the LMC fields and in old LMC globular clusters. Their period distribution and mean periods of field LMC RR Lyrae agree with those measured by Alcock et al. (2000). However, we note that the LMC globular cluster RR Lyrae show a different period distribution, peaked at shorter periods both for RRab and RRc stars. This difference is worth noticing, because it suggests that globular clusters and field RR Lyrae in the LMC do not trace similar populations. Below we will show that there are also differences in metallicities and kinematics.

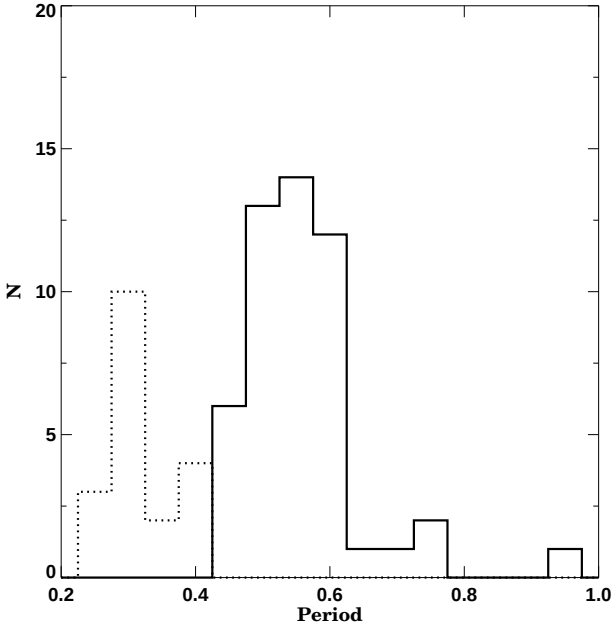

Fig. 2. The period histogram for RR Lyrae stars in our fields. The solid line stand for RRab stars, RRc and RRe stars are marked with a dotted line.

2.2. Spectroscopy

The spectroscopic observations were taken with the FORS1 multi-slit spectrograph at the ESO Very Large Telescope (VLT) Unit Telescope 1 (UT1), during the nights of 10 and 11 January 2003. We used the GRIS_600B+12 grating, that gives $R = 1000$ and covers from λ3500 to λ5900Å. This resolution is adequate for the measurement of radial velocities even in the broad-lined RR Lyrae spectra, provided that a good S/N is achieved.

Table 1. The centers of the observed fields. The Log of the observations.

Event	RA	DEC	MJD(SOFI)	ExpTime (min)	No of Exp.	Date(FOR1)	ExpTime (min)	No of Exp.	RRLyr's
LMC-1	05:14:44.3	-68:48:01	51594.107748	20	2	10.1.2003	20	2	23
LMC-4	05:17:14.6	-70:46:59	51594.129148	20	2	11.1.2003	20	2	13
LMC-7	05:04:03.4	-69:33:19	51594.204557	20	2	11.1.2003	20	2	5
LMC-9	05:20:20.3	-69:15:12	51594.172106	20	2	11.1.2003	20	2	13
LMC-12	05:33:51.7	-70:50:59	51594.214012	20	2	12.1.2003	20	2	8
LMC-14	05:34:44.0	-70:25:07	51594.254683	20	2	12.1.2003	20	2	13

In total, two exposures of 20 minutes were obtained for each mask containing 5-10 RR Lyrae stars. As the FORS1 multi-slit spectrograph can take spectra of up to 19 objects simultaneously, we placed LPV and Cepheid variables on the remaining slits. We observed 58 RR Lyrae, 5 Cepheids, and 23 Miras of the LMC. The spectra of RR Lyrae variables are shown in Fig. 3. The spectra of Cepheid stars and LPV's are shown in Fig. 4 and Fig. 5.

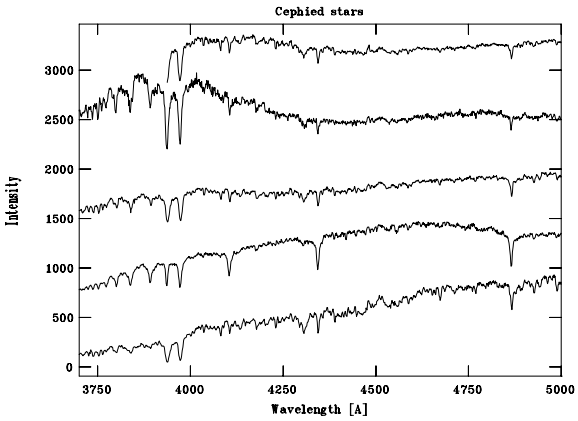

Fig. 4. Spectra of Cepheid stars obtained with FORS1 in Jan. 2003.

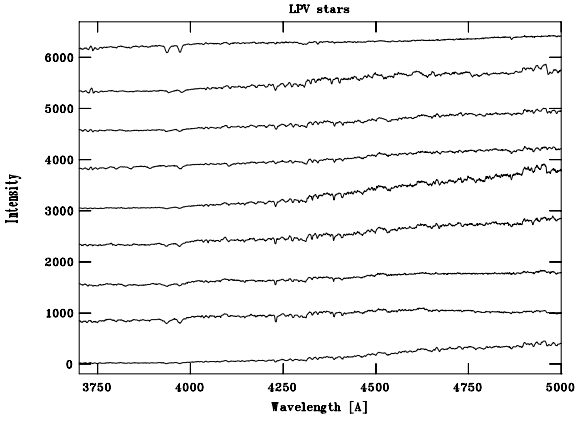

Fig. 5. Spectra of OGLE LPV variables obtained with FORS1 in Jan. 2003.

A substantial fraction of the observing time was devoted to calibrations. Two masks containing RR Lyrae of the globular cluster ω Cen (Clement et al. 2001, Mayor et al. 1997, Kaluzny et al. 1997) were acquired using the same setup. Thus, high quality spectra of 17 ω Cen RR Lyrae (6 RRab, 7 RRc, and 4 RRe) were secured. In addition, a few repeat observations of some of the RR Lyrae stars were taken, in order to assess the velocity errors. The spectra of ω Cen RR Lyrae stars are presented in Fig. 6.

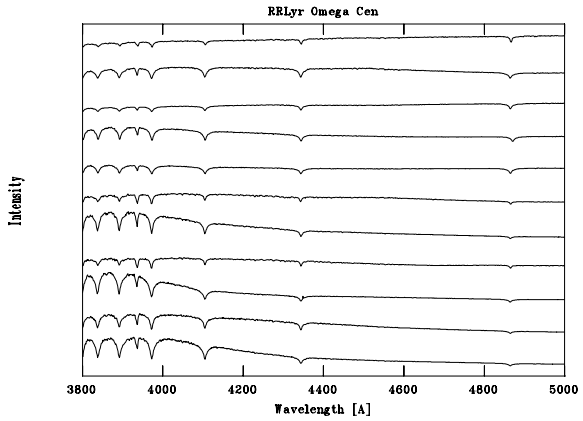

Fig. 6. Spectra of ω Cen RR Lyrae variables obtained with FORS1 in Jan. 2003.

The spectral data were reduced using the standard packages within IRAF. HeNeAr lamps were used for the wavelength calibration, which typically have 14 usable lines that yield 0.2 Å rms. The final extracted and calibrated spectra have on average S/N = 15. This is adequate to measure individual velocities good to about $10-30$ km s^{-1}.

2.3. Photometry

The K-band dataset was obtained with the SOFI infrared imager at the European Southern Observatory's New Technology Telescope; SOFI has a 1024×1024 array with a pixel size of 0.292 arcsec, with a total field of view 5×5 arcmin. We obtained two measurements for each star, in order to define the mean magnitude. The photometry was derived with DAOPHOT II (Stetson 1994), and calibrated with observations of 6 standard stars (Persson et al. 1998). The 1-σ standard deviation of the calibration solution is 0.028 mag. The V and I bands photometry was obtained with WFPC2 on board the HST (P.I. Cook, Alves at al. 2002). The HST photometry is single epoch F555W and F814W WFPC2 observations. Photometry with DAOPHOT II and the standard calibrations to the ground based system result in uncertainties of the order

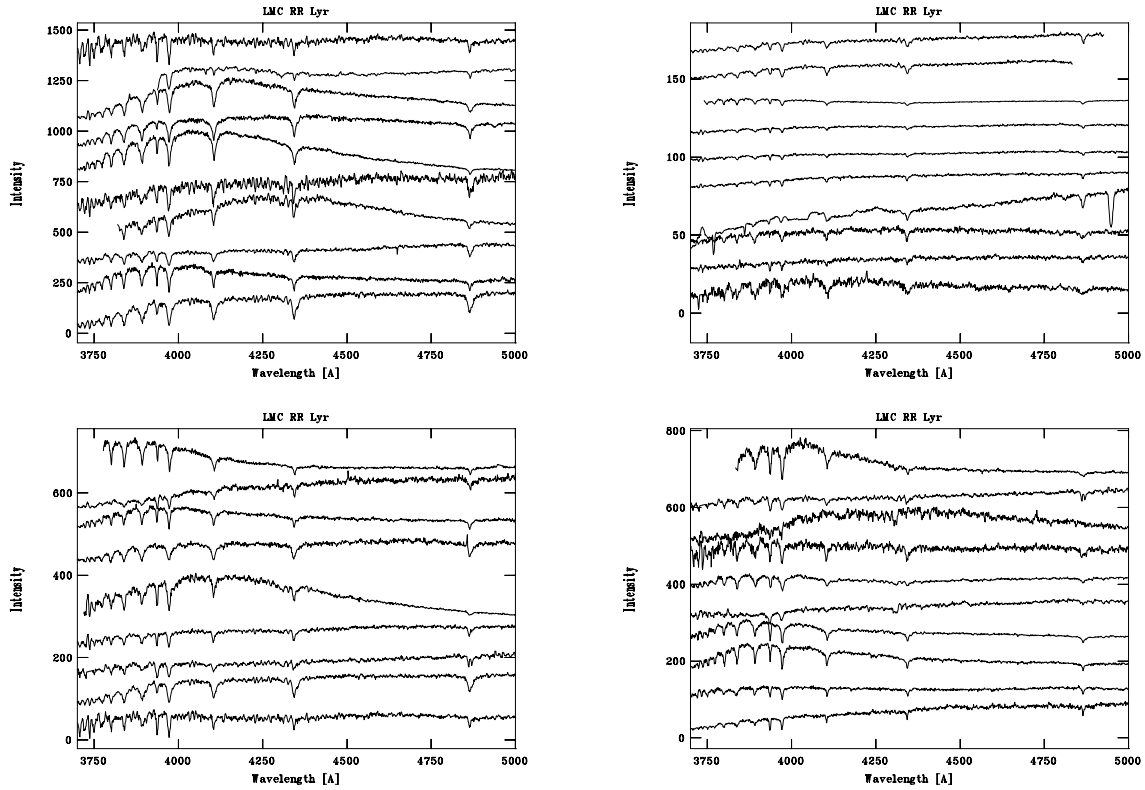

Fig. 3. Spectra of LMC RR Lyrae variables obtained with FORS1 in Jan. 2003.

of 0.02-0.03 mag. The details of the data reduction, error and completeness analysis of the IR and HST photometry are given in Alves at al. (2002).

3. Color - magnitude diagrams

Fig. 7 shows the K,$(V-K)$ color-magnitude diagram (CMD). Well populated red giant branch (RGB) up to $K = 12.5$ and $V - K = 4.2$ and red clump (RC) at $K = 17$ are clearly visible. The variables from our sample, which have K measurements are superimposed: the open circles mark Cepheid stars, the LPV stars are shown as squares, solid circles indicated RRab Lyrae stars, crosses are for RRc stars and triangles are for Red Giant Branch stars + RR Lyrae (RGB+RR Lyr) blends. Everywhere in this paper we use optical mean V, I and R magnitudes of variable stars, taken from the MACHO and OGLE databases. The LPV stars are located at the tip of the giant branch, RR Lyrae and Cepheid stars are located within the Cepheid instability strips. Because of the difference between FORS1 multi-slit spectrograph (6.8× 6.8 arcmin) and SOFI NTT fields (5× 5 arcmin) only part of the stars with spectra have K magnitudes. In total we have the K band magnitudes for 38 RR Lyrae stars, 5 Cepheids and 12 LPV stars from MACHO database. Since we are using V and I mean magnitudes of the variable stars taken from MACHO and OGLE databases there is possibly a systematic error of up to 0.10 mag, because of the differences between MACHO and OGLE V and I mean magnitudes of the variable stars and HST V and I photometry.

Cross-identification with the OGLE database yields 70 additional variables in these fields. On the $(K, I-K)$ color-magnitude diagram (Fig. 8) they are overploted with large open circles. As can be seen most of them are bright LPV stars. Unfortunately, in OGLE database we could not find accurate classifications, periods or amplitudes of these stars.

Several OGLE variable stars lie well below the LMC red giant branch on Fig. 8. They are at the limit of the I-band photometry, and thus probably mismatched variables or noisy measurements.

3.1. Boundaries of the instability strip

The knowledge of the precise location of the RR Lyrae zone is a good test for the stellar pulsation theory. Using the calibration of Montegriffo et al. (1998) we calculated the effective temperature and bolometric magnitude of RR Lyrae stars which have $(V-K)$ colors and K magnitudes. We assume E(B-V)=0.11 (Clementini et al. 2003). A plot of $(K_0, (V-K)_0)$ and (M_{bol}, Log T_{eff}) of these variables is show on Fig. 9. Open circles are for RRab stars, crosses stand for RRc stars. The theoretical value of the blue edge of the RR Lyrae instability strip is located near the $T_{eff} = 7400K$ (Smith 1995), while the red edge is near 6100 K (dashed lines on Fig. 9). Our calculations are in good agreement with the limit for the red edge: we

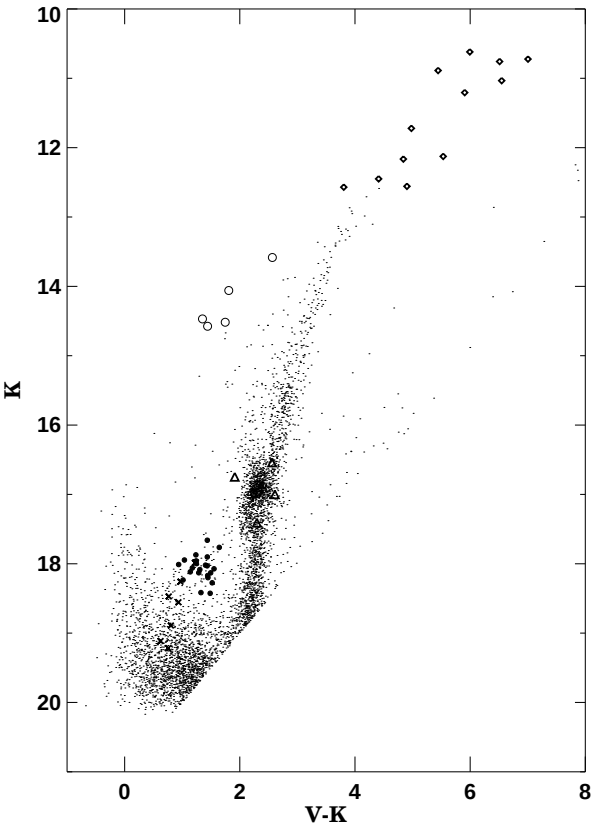

Fig. 7. The K,$(V-K)$ color-magnitude diagram of LMC fields with MACHO variables overploted. The open circles are Cepheid stars, LPV stars are shown as squares, solid circles and crosses indicate RRab and RRc stars and triangles are for RGB+RR Lyrae blends.

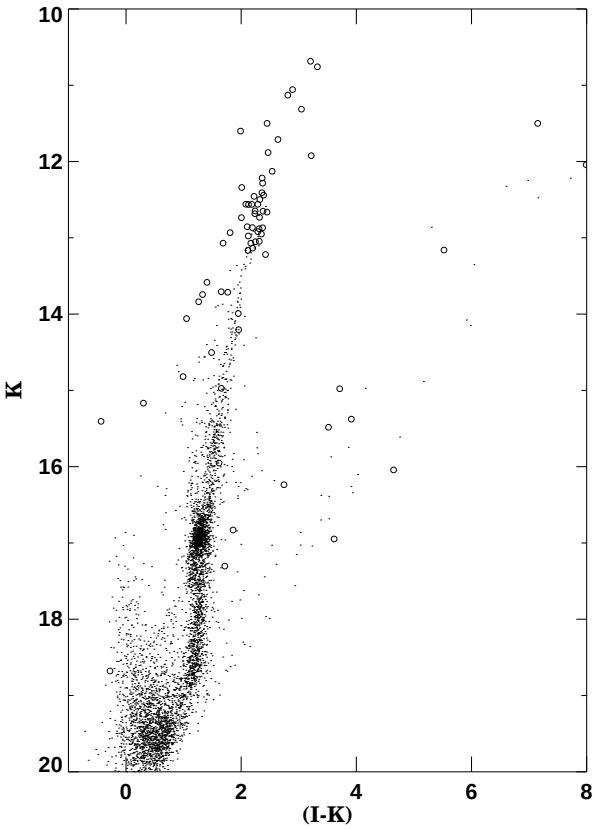

Fig. 8. The K,$(I-K)$ color-magnitude diagram of LMC fields with OGLE variables overploted.

calculated $T_{eff} = 6150K$. For the blue edge, however we have five stars which are hotter, than the theoretical blue limit. Careful check of these stars show that three of them could be anomalous - one is an RRab with large period: P=0.616 days and relatively small amplitude: $A_V = 0.369$ mag, two are RRc stars with larger than usual amplitudes in both V and R: $A_V = A_R = 0.78$. Taking into consideration the errors of our $V-K$ colors and calibration to the theoretical plane, we estimate the error of our T_{eff} determination to be approx. 100K. Since our mean K-band magnitudes are based on two random measurements, this can add additional uncertainty of appox. 0.15 in colors or 250K in temperature. Thus we calculate for the blue edge $7550 \pm 270K$.

3.2. Period-Amplitude relations

The period–amplitude diagram, known as the Bailey diagram, is a widely used tool for analyzing features of RR Lyrae stars. Empirical and theoretical studies suggest that the distribution of RR Lyrae stars in the Bailey diagram depends on their metallicity. The period - A_V (from MACHO databases) amplitude diagram of the RR Lyrae stars in our fields is shown in the left panel of Fig. 10. Since we have only two K images per fields, it was not possible to determine the K band amplitudes. In general, there is a clear separation between RRab (open circles), RRc (crosses) and RRe (filled squares). Fundamental mode RR Lyrae stars present an anti-correlation between the period and amplitude, which seems to be linear. Soszynski et al. (2003) found non-linearity in these diagrams using approx. 7600 RR Lyrae stars in the LMC. Our result is probably due to our small sample (only 70 stars). The width of the sequence is believed to be an effect of a spread in the metal content, which means that our sample has a relatively small metallicity spread. For RRc stars, we also found a weak anti-correlation of amplitudes and periods (Soszynski et al. 2003).

In the middle and right panels of Fig. 10 the (V-K) color - LogP and the (V-K) color - A_V amplitude diagrams are shown. In general, these relations follow the same trends as amplitudes, although they are not so clearly visible, forming overlapping sequences.

According to the theoretical predictions of Bono et al. (1997) the luminosity amplitude depends marginally on the metallicity up to [Fe/H]=0.7 dex. For more metal-rich stars an increase in the metallicity causes a decrease in the amplitudes.

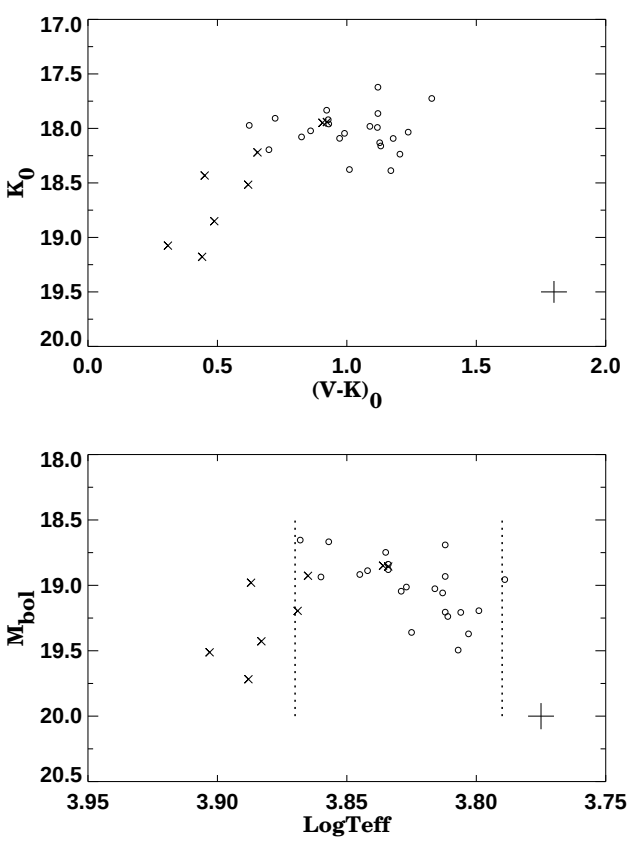

Fig. 9. Top panel: A plot of $(V-K)_0$ vs. K_0 of the RR Lyrae stars with K-band magnitudes. Open circles are for RRab stars, crosses stand for RRc stars. Bottom panel: A plot of Log T_{eff} vs. M_{bol}. The dashed lines represent theoretical limits of the blue and red edges as given in Smith (1995). The crosses represent the typical errors of the photometry and transformation to the theoretical plane.

Our sample was derived from a preliminary classification of MACHO variables. Subsequent analysis has shown MACHO star 11.8750.1425 is not an RRab, while MACHO star 80.648.3667 is an RRab (Alcock et al. 2003). MACHO star 2.5507.6257 has not been confirmed to be an RRc, nor has MACHO star 11.8750.1425. These stars are omitted from the plots and calculations in the following sections.

3.3. Period-luminosity relations

The average apparent luminosities (coming from MACHO databases) of 70 RR Lyrae stars is $< V >= 19.45 \pm 0.04$ and average K luminosities of 33 RR Lyrae stars is $< K >= 18.20 \pm 0.06$. The RGB+RR Lyrae blends are not used for this calculation. The average MACHO database V luminosity of our sample is in agreement with Clementini et al (2003) determination ($< V >= 19.412$) with a systematic shift of 0.038. Fig. 11 shows V_0 vs. LogP and K-band vs. LogP, with magnitudes corrected for reddening. RRab Lyrae star are shown with solid circles, the RRc

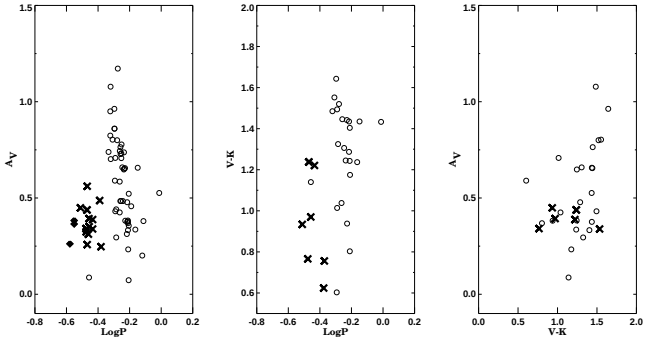

Fig. 10. Left panel: The relation between V amplitudes and Log P for RR Lyrae stars. Open circles are for RRab stars, crosses for RRc stars and filled squares for RRe stars. Middle and right panels: The relations between $V-K$ color and Log P and A_V. The symbols are the same as above.

stars with open ones. Since the sample of RRc stars is limited, their periods are fundamentalized. There is no obvious relation between V_0 magnitude and LogP, while the RR Lyrae K band magnitudes show a well defined linear trend. Bono et al. (2001) published a new theoretical near-infrared Period-Luminosity-Metallicity relation and more recently it was improved on the basis of up-to-date pulsating models (Bono et al. 2003). The predicted theoretical relation for fundamental mode pulsators (solid line) is overploted on Fig. 11. The dashed line represents the best fit for RRab and fundamentalized RRc stars obtained using all data, the thin line is the same fit after the three faint outliers and RRab star with very large period were excluded. The agreement with Bono et al. (2003) prediction is good, when we exclude these four outliners. Following the same procedure as in Bono et al. (2001) we calculated $M_K = 0.332$ at LogP= -0.30, obtaining an infrared distance modulus of $\mu_0(K) = 18.48 \pm 0.08$. Here, we adopted $E(B-V) = 0.11$ (Clementini et al 2003) and [Fe/H] $= -1.46$ dex (see Sec 8) and luminosity $\log(L/L\odot) = 1.72$. The calculated distance is comparable within the errors with most of the LMC distance determinations from the literature.

4. Radial Velocities

It is well known (Smith 1995) that the line spectrum of RR Lyr star undergoes a cyclic change during the pulsation cycle. The observed radial velocity depends also upon which spectral lines are measured. In some phases of the pulsation cycle, the velocities based on measurements of the Balmer lines are systematically different from those based on metallic lines. The reason is that lines of different elements and ionization states arise from different levels within the moving stellar atmosphere. The difference is largest during rising light. The difference in the radial velocities of lines that form at high and low optical depths is due to a radial velocity gradient. This phenomenon also

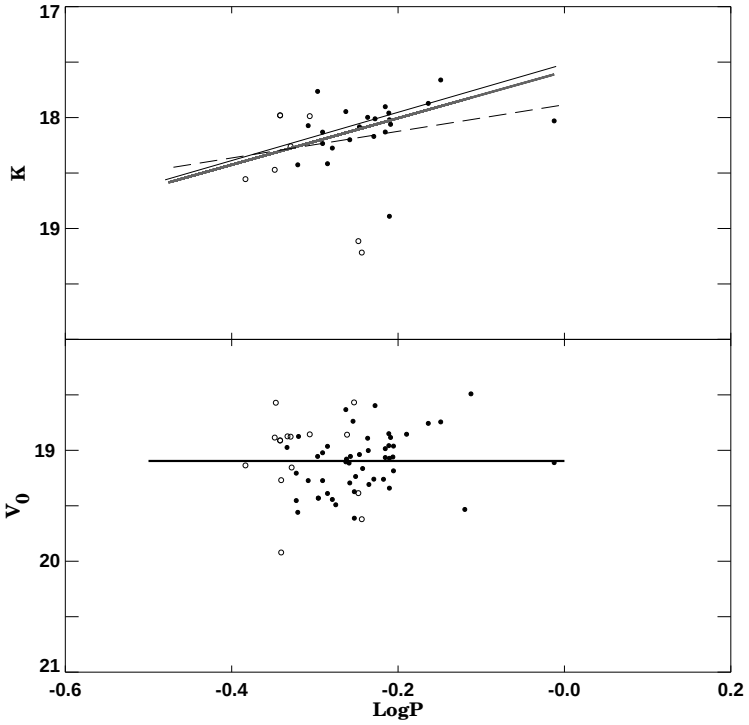

Fig. 11. Top panel: LogP vs. K plot for RRab stars (sold circles) and RRc (open circles) in the LMC. The Bono et al. (2003) relations are shown with solid lines. The dashed line is a best fit for RRab and fundamentalized RRc stars, the thin line represent the best fit, without the four outliers. Bottom panel: LogP vs. V_0 plot for RRab (solid circles) and fundametalized RRc (open circles) in the LMC. The solid line is the average magnitude. The adopted distance module, reddening and metallicity are 18.48, 0.11 and −1.48, respectively.

causes a systematic shift in the phase of maximum velocity (Bono et al. 1994).

There are two commonly used techniques to measure radial velocities: cross-correlation technique, which computes the radial velocities via Fourier cross correlation, and by centroiding the individual spectral lines. We measured the radial velocities of our sample using both of these techniques. The comparison between radial velocities measured by two methods for ω Cen RR Lyrae stars is shown on Fig. 12. The cross-correlation velocities are corrected for heliocentric velocity and are shifted to the mean velocity of ω Cen $RV_{mean} = 232.78 \pm 13.7$ km s^{-1} (Mayor at al. 1997). In general, the agreement is good, except for a few cases with larger differences. We calculated the phases of all RR Lyrae stars at the moment of our observations using ephemeredes, amplitudes and periods from Kaluzny et al. (1997). As expected, these outlying stars (V266, V88, V271, V275 and V267 see Table 2) are around maximum light and the radial velocities of CaII-lines are significantly different from those of H-lines. In general, the two techniques yield similar results within 15 km s^{-1}, but the individual errors of measurements are larger when we use the cross-correlation technique. The result is not surprising, taking into account the relatively broad lines of RR Lyrae stars.

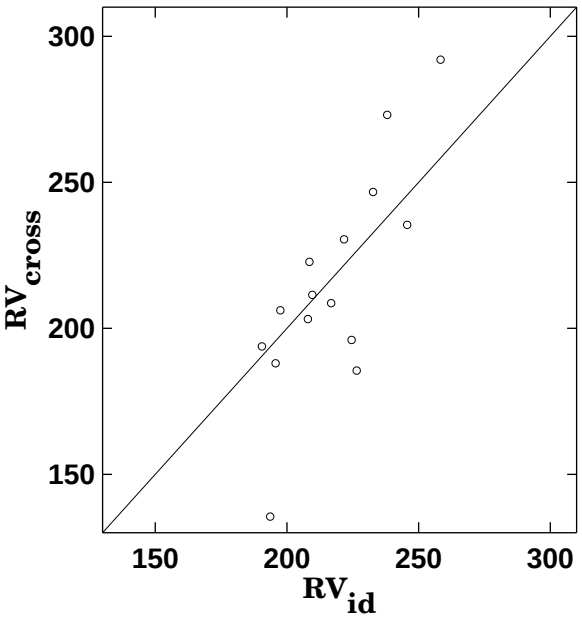

Fig. 12. Radial velocities in km s^{-1} of ω Cen RR Lyrae variables measured by Fourier cross correlation and by centroiding the individual spectral lines techniques.

Therefore, we prefer to measure the radial velocities as an unweighted mean value of individual radial velocities of Hβ, Hγ, Hδ, and CaII K λ3933.66 Å, excluding the Ca line velocities in the cases of rising light. We measured radial velocities of 58 RR Lyrae stars, 5 Cepheids and 33 LPV's stars in our six LMC fields. The internal errors measured from the different lines range from 1 to 33 km s^{-1}.

The pulsation of a RR Lyrae star induces a periodic variation in the radial velocity of the star. The radial velocity curve roughly reflects the light curve, with minimum radial velocity coming at maximum visible light for RRab variables. For RRc stars the maximum radial velocity is reached about 0.1 of a cycle after maximum light. The velocity amplitudes for RRab stars are between 60-70 km s^{-1}. and for RRc stars are between 30-40 km s^{-1} (Smith 1995). Therefore, it is necessary to correct such measured radial velocities for this large velocity amplitude through their cycle of pulsation. Liu (1991) derived a correlation between the pulsational velocity vs. V light amplitudes for RRab stars. Unfortunately, we have only 6 RRab stars in our control sample of ω Cen RR Lyrae's and two of them have only one line measured accurately. We used the Liu (1991) calibration to correct the raw velocities of these four stars and to estimate how the velocity dispersion will change after the correction. The mean value of measured radial velocities is $RV_{mean} = 247 \pm 29$ km s^{-1}. The pulsation amplitudes are between 67 and 83 km s^{-1} and the

Table 2. ω Cen RR Lyrae stars

Name	OGLE	$< V >$	A_V	Period	Type	RV	σ_{RV}	Phase	RV_{corr}
V139	118	14.35	0.71	0.6768	RRab	278	4	0.09	282
V111	136	14.46	0.60	0.7629	RRab	228	16	0.16	238
V118	109	14.43	1.00	0.6116	RRab	218	27	0.54	263
V88	210	14.23	0.67	0.6904	RRab	266	13	0.97	273
V144	112	14.41	0.48	0.8352	RRab	239	–	0.75	275
V113	128	14.41	1.20	0.5733	RRab	148	–	0.76	209
V273	139	14.60	0.39	0.3672	RRc	237	3	0.09	–
V153	140	14.55	0.44	0.3863	RRc	245	15	0.24	–
V264	108	14.75	0.45	0.3214	RRc	211	5	0.26	–
V145	130	14.56	0.44	0.3732	RRc	230	10	0.36	–
V157	138	14.56	0.45	0.4066	RRc	247	13	0.66	–
V275	149	14.50	0.34	0.3782	RRc	214	17	0.80	–
V271	132	14.44	0.43	0.4431	RRc	229	12	0.97	–
V119	106	14.65	0.29	0.3059	RRe	216	2	0.26	–
V166	142	14.54	0.13	0.3414	RRe	242	8	0.51	–
V267	121	14.46	0.25	0.3159	RRe	253	3	0.78	–
V266	115	14.54	0.27	0.3524	RRe	258	6	0.86	–

mean value of the corrected velocities is $RV_{mean} = 264 \pm 19$ km s^{-1}. For RRc stars Liu (1991) says that there should be a similar relation, but he had too few data to derive it. Although the pulsation amplitudes are large since the RR Lyrae are observed in random phase, the velocity dispersion does not change so much. The data for ω Cen stars are summarized in Table 2.

The same test was performed on the sample of RRab stars in the LMC. We used the MACHO database to derive the phases of the stars in the moment of our observations. The mean value of measured radial velocities is $RV_{mean} = 228 \pm 61$ km s^{-1}, the mean value of the corrected velocities is $RV_{mean} = 252 \pm 58$ km s^{-1}. The difference in the velocity dispersions for corrected and un-corrected radial velocities is small.

We decided to use un-corrected radial velocities for the calculation of the velocity dispersion for the whole sample, rather than correcting only part of the sample. The comparison of the velocity dispersion of RR Lyrae in the LMC with the other stellar populations will then be used to test for the presence of a stellar halo around the galaxy.

The data for the LMC RR Lyrae stars and Cepheids are summarized in Table 3, and in Table 4 we list the radial velocities of OGLE LPVs.

In columns 2,3,4 and 5 of Table 3 are mean V magnitude, amplitude, period of the pulsation and type of the star taken from MACHO database. Note uncertain/wrong classification of 11.8750.1425,80.6468.3667 and 2.5507.6257 (see Sec 3.1 and 3.2).

Table 3. LMC RR Lyrae and Cepheid stars

MACHO name	$< V >$	A_V	Period(d)	Type	RV (km/s)	σ_{RV}
10.3802.311	18.99	0.43	0.5460	RRab	182	10
10.3802.339	19.37	0.71	0.5120	RRab	173	6
10.3802.446	19.49	0.45	0.3080	RRc	82	13
10.3922.978	19.09	0.48	0.5568	RRab	315	–
10.3923.351	19.24	0.34	0.3340	RRc	144	19
11.8622.757	19.11	0.34	0.6860	RRab	178	18
11.8623.3792	19.31	0.38	0.6149	RRab	187	11
11.8623.779	19.20	0.38	0.6150	RRab	196	11
11.8623.826	18.95	0.38	0.5902	RRab	288	20
11.8743.1422	20.27	0.56	0.3396	RRc	179	11
11.8744.658	18.92	0.25	0.4155	RRc	312	8
11.8744.752	19.14	0.37	0.2809	RRe	210	9
11.8744.830	19.47	0.48	0.5510	RRab	330	19
11.8749.1208	19.56	0.82	0.4757	RRab	257	23
11.8749.1324	19.63	0.43	0.5120	RRab	282	–
11.8750.1425	19.26	0.09	0.3490	RRab	270	28
11.8750.1672	19.62	0.26	0.3400	RRc	231	14
11.8750.1827	19.74	0.30	0.5186	RRab	233	11
11.8750.2045	19.81	0.95	0.4763	RRab	267	33
11.8870.1275	19.33	0.74	0.4638	RRab	247	19
11.8871.1096	19.43	0.74	0.5473	RRab	291	–
11.8871.1122	19.71	0.70	0.5010	RGB+RR	294	–
11.8871.1299	19.61	0.56	0.5960	RGB+RR	233	22
11.8871.1362	19.61	0.31	0.6064	RRab	339	8
11.8871.1447	19.59	0.26	0.2640	RRe	148	6
11.8871.1516	19.46	0.59	0.5463	RRab	309	–
13.5839.1023	19.66	0.65	0.5823	RRab	219	–
13.5840.608	19.32	0.44	0.5188	RRab	234	14
13.5840.730	19.41	0.07	0.6215	RRab	228	24
13.5960.884	19.23	0.31	0.3459	RRc	183	11
13.5962.547	19.21	0.46	0.6464	RRab	207	14
13.6082.701	19.41	0.73	0.5525	RRab	214	8
2.5507.5945	19.54	0.52	0.6234	RRab	256	10
2.5507.6046	19.63	0.80	0.4920	RRab	338	31
2.5508.3096	19.96	0.71	0.5593	RRab	149	29
2.5628.5690	19.69	0.37	0.6156	RRab	144	18
2.5628.6276	19.91	1.08	0.4781	RRab	135	–
79.5507.1039	19.59	0.78	0.5608	RRab	238	14
79.5507.1485	19.31	0.36	0.6234	RRab	261	9
79.5507.1580	19.46	0.53	0.9720	RRab	209	1
79.5508.427	19.73	0.73	0.5593	RRab	200	15
79.5508.534	19.52	0.48	0.5723	RRab	169	–
79.5508.682	19.89	0.20	0.7591	RRab	161	13
79.5508.735	19.78	0.86	0.5057	RRab	215	–
79.5628.1065	19.84	1.17	0.5305	RRab	274	19
79.5628.1300	19.42	0.33	0.6160	RRab	280	–
79.5628.1597	19.51	0.38	0.2812	RRe	179	3
79.5628.1650	19.26	0.44	0.3389	RRc	147	–
79.5628.2110	19.80	0.80	0.5260	RRab	247	–
80.6347.1940	19.21	0.49	0.4083	RRc	184	14
80.6467.2128	19.35	0.74	0.5805	RRab	151	14
80.6468.1883	18.92	0.32	0.3346	RRc	266	11
80.6468.2616	19.21	0.39	0.3684	RRc	199	11
80.6468.3667	20.05	1.19	0.4308	RRc	101	1
80.6469.1657	19.24	0.65	0.5804	RRab	122	12
80.6469.1712	18.84	0.38	0.7720	RRab	232	–
80.6588.2703	19.23	0.70	0.4794	RRab	259	–
80.6589.2425	19.51	0.35	0.3497	RRc	198	11
80.6348.23	15.70	0.37	4.7348	Cep	328	–
80.6468.21	15.52	0.12	3.1557	Cep	285	6
80.6468.46	15.82	0.58	3.3587	Cep	278	6
11.8622.24	15.90	0.24	2.0921	Cep	241	34
11.8870.40	16.26	0.59	2.9827	Cep	236	10

Table 4. LPV stars from OGLE database

OGLE name	RV (km/s)	σ_{RV}
OGLE05145362-6846533	214	39
OGLE05145091-6850289	247	10
OGLE05145362-6846533	272	–
OGLE05144133-6848591	261	17
OGLE05143819-6849131	223	40
OGLE0514363-6849378	269	27
OGLE05143421-685033	193	31
OGLE05144922-684628	160	–
OGLE05144133-6848591	238	1
OGLE05143815-6849217	226	34
OGLE05143443-6849511	207	13
OGLE05143421-685033	218	29
OGLE05041263-6931104	164	17
OGLE0504633-6931282	203	49
OGLE05041042-6931483	193	34
OGLE0504966-6932445	224	31
OGLE05202161-6912358	81	–
OGLE05201061-6913378	243	36
OGLE05202958-6914441	218	–
OGLE05201862-6916558	344	2
OGLE05202644-6913122	47	2
OGLE0520061-6913378	143	78
OGLE05202958-6914441	253	32
OGLE05202789-691596	211	32
OGLE0520484-691531	201	37
OGLE05202923-6915589	277	50
OGLE05203023-6916347	206	4
OGLE05202042-6917356	399	–
OGLE05344257-702531	261	26
OGLE05343669-7027283	151	–
OGLE05343389-7027361	213	–
OGLE05345159-7026341	275	–
OGLE05344708-7025235	294	–
OGLE0534446-7027311	174	35

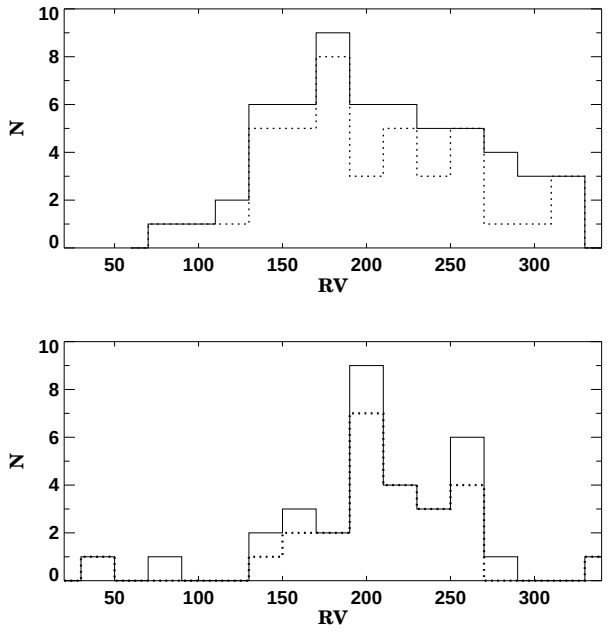

Fig. 13. The radial velocity histogram for RR Lyrae stars (top panel) and LPVs (bottom panel) in our fields. The dotted lines are for the selected sample of stars, solid lines marked the whole sample (see text).

We discarded 15 RR Lyrae stars that have only one line measured accurately, leaving 43 stars that have 2-4 lines accurately measured. Of the final 43 stars considered, 29 are RRab, 11 are RRc and 3 are RRe according to the MACHO light curves. The same analysis was performed for LPV stars - here we have 23 stars with accurately measured velocities.

In the Fig. 13 the histogram of radial velocities of the whole sample of RR Lyrae and LPV stars are plotted with the solid lines and the selected samples, with the best measured velocities, are shown with the dotted lines. As can be seen the distributions are similar.

For the LMC RR Lyrae we measure $\sigma_{obs} = 61$ km s^{-1} and $\sigma_{true} = 53$ km s^{-1} (Minniti et al. 2003). This is larger than the velocity dispersion of other populations: $\sigma_{true} = 28$ km s^{-1} for the LMC LPV stars, $\sigma_{true} = 24$ km s^{-1} for Cepheids and $\sigma_{true} = 19$ km s^{-1} for ω Cen RR Lyrae stars. This large velocity dispersion of $\sigma_{true} = 53$ km s^{-1} implies that RR Lyrae stars are distributed in a halo population as discussed in (Minniti et al. 2003).

In order to estimate the stability of the measured dispersion, we divide the sample in different sub samples. For the best N=29 RRab stars, $V_{mean} = 228$ km s^{-1}, $\sigma = 60$ km s^{-1}; for all N=43 RRab stars, $V_{mean} = 233$ km s^{-1}, $\sigma = 57$ km s^{-1}; for the best N=11 RRc stars, $V_{mean} = 189$ km s^{-1}, $\sigma = 67$ km s^{-1}; for all RRc stars, $V_{mean} = 186$ km s^{-1}, $\sigma = 65$ km s^{-1}.

In Fig. 14 we present radial velocity cumulative distributions of different LMC population as measured from our spectra. The solid line represents LMC RR Lyrae stars, the thin line is for Mira stars. Kolmogorov-Smirnov (KS) comparison of two data sets gives the maximum difference between the cumulative distributions, $D = 0.26$ with a corresponding $P = 0.20$. KS finds that the LMC RR Lyrae stars distribution is consistent with a normal distribution $P = 0.99$ where the normal distribution has mean 217.8 ± 64 km s^{-1}. KS finds that the Mira stars distribution is consistent with a normal distribution $P = 0.64$ where the normal distribution has 229 ± 51 km s^{-1}. The comparison between the ω Cen RR Lyrae stars and the LMC RR Lyrae stars shows the maximum difference between the cumulative distributions: D is 0.5102 with a corresponding P of: 0.003. In the other words we have statistically significant difference with respect to ω Cen RR Lyrae stars and more data are necessary to confirm or reject the hypotheses of difference between the LMC Mira and RR Lyrae stars.

In general, the amount of rotation compared with the velocity dispersion determines whether a population is kinematically hot, $V/\sigma << 1$, as opposed to kinematically cold, $V/\sigma \sim 1$. The LMC RR Lyrae appear to belong to a kinematically hot population, the present data is insufficient to measure the rotation. The mean velocities are less precise than the velocity dispersion, as seen by comparing the different mean velocities of the Miras, RR Lyrae, and Cepheids. While there may be a hint of rotation for the RR Lyrae based on the sample of the best 43 stars, this signature disappears when we include the extended sample of 58 stars. In order to test how the rotation affects the velocity dispersion, we computed the dispersions independently for the different fields. The results are given in Table 5. In column 2 we put the number (N_{sel}) of the stars with the "best" radial velocity measurements, columns 3 and 4 give their mean velocity (RV) and dispersion (σ_{RV}),

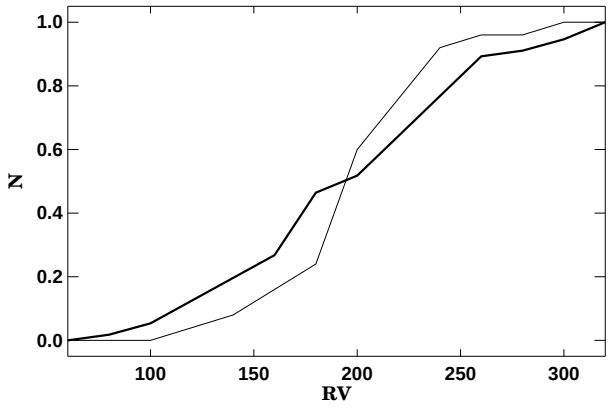

Fig. 14. The radial velocity cumulative distributions of different LMC population as measured from our spectra. The solid line represents the LMC RR Lyrae stars, the thin line is for Mira stars.

Table 5. Mean radial velocity and dispersion for several fields in LMC

Field	N_{sel}	RV	σ_{RV}	N_{all}	RV	σ_{RV}
10	4	145	45	5	179	85
11	17	241	55	21	251	54
13	5	213	20	6	214	18
2	4	222	93	5	204	90
79	7	217	42	12	215	45
80	7	260	25	95	274	37

while next three columns N_{all}, RV and σ_{RV} are for the whole sample of stars.

The field with the largest number of RR Lyrae, Field 11, provides the most accurate and stable measurement. The observed $\sigma = 55$ confirms that the RR Lyrae have larger velocity dispersion than all other measured populations, even though it is slightly smaller than the overall dispersion observed, $\sigma = 61$. Clearly, more data are needed in order to estimate the rotation component.

In addition, we must point out a difference in the published rotational centers of the LMC, which bears on the measurement of the rotation of the various populations. For example, van der Marel et al. (2002) obtain $RA = 5^h29\overset{m}{.}1$, $DEC = -69°47'$, while Alves & Nelson (2000) obtain $RA = 5^h19\overset{m}{.}6$, $DEC = -69°58'$. The RR Lyrae maps of Soszynski et al. (2003) indicate that the center of the field RR Lyrae distribution in the LMC is located at: $RA = 5^h22\overset{m}{.}9$, $DEC = -69°39'$, offset from these previous determinations.

5. Metallicities

Preston's (1959) ΔS method is a classical method for determining RR Lyrae abundances from low resolution spectra. It measures the difference in spectral type between the CaII K line and the H ($H_\delta, H_\gamma, H_\beta$) lines relative to spectral type standards of approximately solar abundance. Several modifications of the method can be found in the literature – Butler (1975), Freeman & Rodgers (1975), Smith (1995), Clementini at al. (2003). Layden (1994) adopted Freeman & Rodgers (1975) method, which uses the equivalent width (EW) of the CaII K-line (W(K)) and the H-lines (W(H)) to estimate abundances but does not explicitly convert these measurements to spectral types. He derived the relation between W(K), W(H) and metallicities [Fe/H] on the Zinn & West (1984) scale for 142 field RRab Lyrae stars in our Galaxy. Equation 7 given in Layden (1994) is :

$$W(K) \; = \; a + b \times W(H) + c \times [Fe/H] + d \times W(H) \times [Fe/H]$$

where W(K) and W(H) are the equivalent widths of CaII K-line and H-lines respectively, and [Fe/H] is the metallicity in Zinn & West (1984) scale. The a, b, c, and d coefficients are given in Table 8 of the paper for three different cases. The first one calibrates [Fe/H] vs. EW without correction for interstellar contribution to the K line. To avoid the metal line contamination of H_β in the second case, Layden (1994) uses only H_δ and H_γ to measure the EW of H-lines. And finally in the third one he adds the H_β line, after performing the corrections.

Since we did not observe enough standard stars for calibration, we used the above equation to determine the [Fe/H] of LMC RRab Lyrae stars. Following Layden's (1994) three step approach, first we measured pseudo-equivalent widths of CaII K line and $H_\delta, H_\gamma, H_\beta$ lines. We used the SPLOT routine in IRAF, fitting the spectral lines with a Voigt profile. The pseudo-EWs were computed by dividing the instrumental fluxes within a small spectral region centered on the selected feature, with the continuum. For RRab stars, the phases of rising light are to be avoided because of the effects of shock waves and/or rapidly changing surface gravity. Using light curves from Kaluzny et al. (1997) for ωCen stars and from the MACHO database for LMC RR Lyrae's we calculated the phases of variable stars at the moment of our observations and rejected all the stars which had phases greater than 0.75. No correction for interstellar contribution to the K line was made, because the resolution of the spectra is not sufficient to separate stellar and interstellar component. To correct the metal line contamination of H_β line, we inspected the line profiles for signs of line doubling or for anomalously broad, shallow shapes. In these cases we calculated [Fe/H], using only mean value of H_δ and H_γ and the second coefficients of Layden's calibration.

We observed 17 RR stars in ωCen, but only 6 of them are RRab stars. The stars V88 and V111 (Clement et al. 2001 classification) have no CaII K line in their spectrum, the star V144 was observed in two masks, one of them is at phase 0.75. All these stars have [Fe/H] values measured by Butler et al. (1978) from low resolution spectra by classical ΔS method and by Rey et al. (2000), which calibrated hk index of the $Caby$ photometric system vs. metallicity. The mean differences between Rey et al. (2000) metallicities of

these stars and our measurements is 0.11 ± 0.32, between Butler et al. (1978) measurements and ours is 0.01 ± 0.07, Rey et al. (2000) and Butler et al. (1978) metallicities have a differences 0.10 ± 0.36. Taking into account the small correction needed for the interstellar K line we should expect sigma closer to 0.1. We have good agreement with spectroscopic measurements, but large discrepancies with Rey et al.(2000) determination. They discuss the large difference in results from different methods and concluded that ΔS metallicities of ωCen are not accurate. Of course we have only 4 stars, but they support Jurcsik's (1998) suggestion, who also finds significant discrepancy between metallicities obtained from Fourier decomposition of the light curves and the spectroscopic measurements. Jurcsik's conclusion is that it is necessary to obtain high-accuracy spectroscopic observations in order to confirm and understand the nature of this difference.

The EW of the LMC RR Lyrae stars were measured independently by two of us (J.B. and M.R.) and the unweighted mean value and the errors of the mean calculated. The average [Fe/H] value of our 23 RRab Lyrae stars is [Fe/H] $=-1.50 \pm 0.1$ dex. The metallicity of another four stars are calculated from Fourier decomposition of the light curves from Alcock et al. (2003) and are added to the spectroscopic measurements. As a result we have 27 metallicity determinations and the mean value is [Fe/H] $=-1.46 \pm 0.09$ dex. The mean metallicity of RR Lyrae stars is in very good agreement with Clementini et al. (2003) average value [Fe/H] $=-1.48 \pm 0.29$ dex. Thus, the field RR Lyrae stars seem to be more metal rich than globular cluster RR Lyrae star population (Walker 1992). Our metallicities are on the Zinn & West (1984) scale and they would be slightly different on the Carretta & Gratton (1997) scale. This would introduce systematic effects to the distance scale, that have been reviewed elsewhere (e.g. Walker 1998, Walker 2003). Based on these considerations, we estimate a global uncertainty of 0.2 dex in the metallicity.

The individual [Fe/H] determinations are given in Table 6. The distribution over the metallicity is shown on Fig. 15 and seems to fit well Gaussian distribution. Of course, more data are necessary to confirm this.

It is well known that the absolute magnitude of an RR Lyrae star, M_V, is a function of metallicity [Fe/H] (Sandage 1981). Recently, Olech et al. (2003), using new photometry of RRab Lyrae stars in ωCen, derived the relation in the form : $M_V = 0.26 \times$[Fe/H]$+0.89$. Despite the large scatter, in general our data agree with this relation as can be seen in Fig. 16. To calculate M_V, we used the LMC distance modulus of 18.48 determined in Sec. 3 and the reddening of E(B-V)=0.11 (Clementini et al. 2003).

In the M_K,[Fe/H] plot, however, the relation is flatter than in the V band as can be seen on the bottom panel of Fig. 16. The best fit of our 9 points gives: $M_K = 0.05 \times [Fe/H] - 0.31$ dex. There is an indication that the absolute K magnitude is less sensitive to the metallicity.

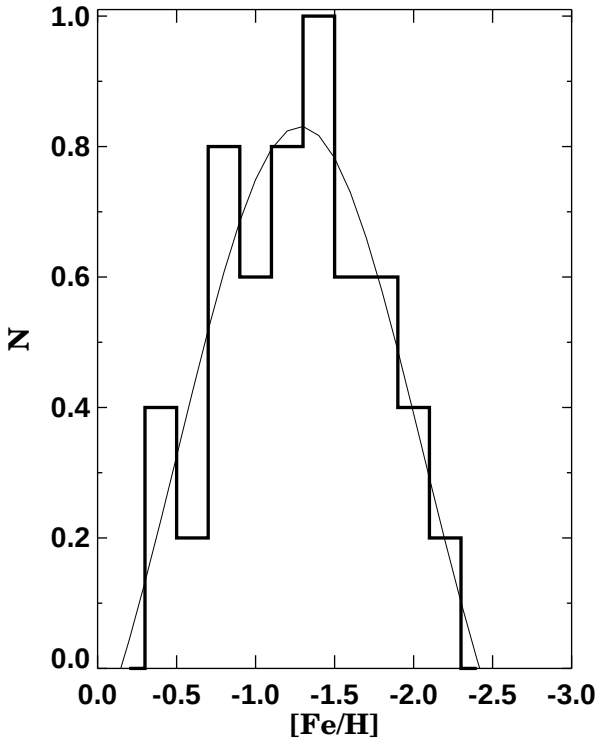

Fig. 15. The metallicity histogram for RR Lyrae stars in our fields. The solid line represents the Gaussian distribution.

6. Conclusions

We measure a velocity dispersion of $\sigma = 53 \pm 10$ km s^{-1} for 43 LMC RR Lyrae. This dispersion indicates a kinematically hot population, similar to the Milky Way, where the RR Lyrae are distributed in the halo. This velocity dispersion is also larger than that of the old LMC globular clusters.

We measure a mean $[Fe/H] = -1.46 \pm 0.09$ dex based on $N = 27$ field LMC RR Lyrae. This measurement agrees with the recent result of Clementini et al. (2003), who found $[Fe/H] = -1.48 \pm 0.29$ dex based on $N = 100$ field RR Lyrae in the LMC. This mean metallicity is different from the globular clusters: Walker (1992) finds $[Fe/H] = -1.9 \pm 0.2$ dex based on $N = 182$ RR Lyrae in seven LMC globular clusters. This difference, coupled with the difference in the kinematics and the period distributions, suggests that field RR Lyrae and globular clusters trace different populations in the LMC.

We measure the mean K-band magnitudes of 37 field RR Lyrae in the LMC, $K = 18.20 \pm 0.06$. Based on this mean magnitude and on the theoretical near-IR period-luminosity-metallicity relations of Bono et al (2001, 2003), we compute an LMC distance modulus $\mu_0 = 18.48 \pm 0.08$.

Acknowledgements. JB, DM, and MR are supported by Fondap Center for Astrophysics 15010003. KHC's work was performed under the auspices of the U.S. Department of Energy, National Nuclear Security Administration by

Table 6. Metallicities, K magnitudes and $V-K$ colors of the LMC RR Lyrae stars.

MACHO name	[Fe/H]	σ	Type	$<K>$	$V-K$
10.3802.311	−1.04	0.01	RRab	17.95	1.04
10.3802.339	−1.13	0.11	RRab	18.23	1.01
10.3802.446	–		RRc	18.56	0.93
10.3922.978	−1.87	–	RRab	–	–
10.3923.351	–		RRc	18.47	0.77
11.8622.757	−2.22	0.11	RRab	17.87	1.24
11.8623.3792	−1.46	0.05	RRab	–	–
11.8623.779	−1.65	0.01	RRab	17.96	1.24
11.8623.826	−0.73	0.02	RRab	18.01	0.94
11.8744.830	−2.14	0.01	RRab	–	–
11.8749.1208	−1.43	0.15	RRab	–	–
11.8749.1324	−2.33	0.06	RRab	18.13	1.49
11.8750.1425	−2.04	0.08	RRab	18.12	1.14
11.8750.1827	−2.10	0.18	RRab	18.42	1.33
11.8750.2045	−0.69	0.04	RRab	–	–
11.8870.1275	−1.67	0.03	RRab	–	–
11.8871.1362	−0.98	0.21	RRab	–	–
13.5840.608	−1.08	0.06	RRab	–	–
13.5840.730	−1.20	0.19	RRab	–	–
13.5840.768	–		RRab	18.20	1.45
13.5961.435	–		RRab	18.24	0.60
13.5961.511	–		RRab	17.66	1.44
13.5961.623	–		RRab	18.06	1.18
13.5961.648	–		RRab	18.08	1.31
13.5961.720	–		RRab	18.13	1.29
13.5962.547	−1.31	0.04	RRab	–	–
13.5962.656	–		RRab	17.90	1.44
2.5507.6046	–		RRab	18.07	1.55
2.5507.6257	–		RRc	18.22	1.53
2.5627.4847	–		RRc	19.22	0.76
2.5628.5690	–		RRab	18.89	0.80
2.5628.6276	−0.57	0.01	RRab	18.43	1.39
79.5507.1485	−1.85	0.11	RRab	–	–
79.5507.1580	–		RRab	18.03	1.43
79.5508.427	−1.66	0.17	RRab	–	–
79.5508.534	−1.31	0.04	RRab	–	–
79.5508.682	−1.92	0.06	RRab	–	–
79.5508.735	−1.51	0.13	RRab	–	–
79.5627.1761	–		RRc	19.11	0.62
79.5628.1065	−1.24	–	RRab	–	–
79.5628.1300	–		RRab	18.02	1.40
79.5628.1650	–		RRc	17.98	1.24
79.5628.2110	–		RRab	18.28	1.52
80.6468.2582	–		RRab	18.17	1.44
80.6468.2616	–		RRc	17.99	1.22
80.6468.2765	–		RRc	18.26	0.97
80.6468.2799	–		RRab	17.76	1.64
80.6468.3667	–		RRc	18.51	1.54
80.6469.1657	−1.90	0.09	RRab	18.00	1.25
80.6469.1712	−-1.61	0.01	RRab	–	–
80.6588.2703	−0.91	0.16	RRab	–	–

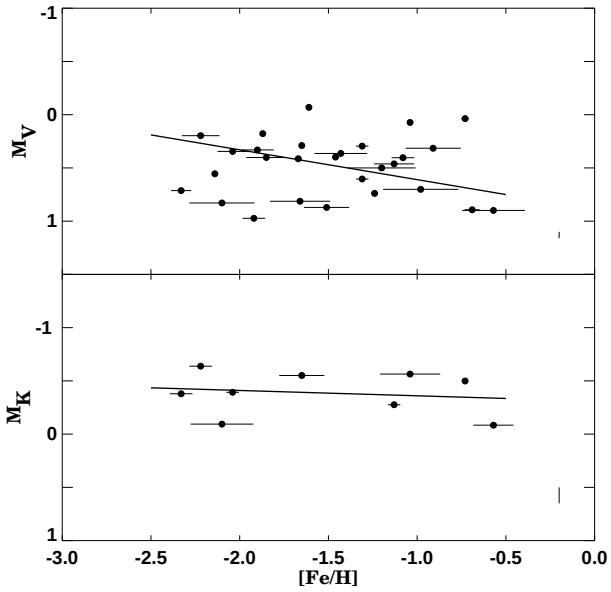

Fig. 16. Top panel: M_V,[Fe/H] plot for RRab stars in LMC. The Olech et al (2003) relation is shown with the solid line. Bottom panel: M_K,[Fe/H] plot for RRab stars in LMC. The solid line is the best linear fit. The vertical lines are the global error of the M_V and M_K magnitudes. The adopted distance modules and reddening are 18.48 and 0.11, respectively (see text).

the University of California, Lawrence Livermore National Laboratory under contract No. W-7405-Eng-48. The authors gratefully acknowledge the comments by the referee Dr. Bono and comments by M. Catelan and H. Smith.

References

Alcock, C., et al. 1996, AJ, 111, 1146
Alcock, C., et al. 2000, AJ, 542, 257
Alcock, C., et al. 2001, Nature,414,617
Alcock, C., et al. 2003, ApJ, 598, 597
Alcock, C., et al. 2004, ApJ, 127, 334
Alves, D., & Nelson, C. 2000, ApJ, 542, 789
Alves, D. R., Rejkuba, M., Minniti, D., Cook, K.H. 2002, ApJ, 573, L54
Bono,G., Stellingwerf R. 1994, ApJS, 93, 233
Bono,G., Caputo,F., Castellani,V., Marconi,M. 1997, ApJ, 479, 279
Bono,G., Caputo,F., Castellani,V., Marconi,M., Storm,J. 2001, MNRAS, 326, 1183
Bono,G., Caputo,F., Castellani,V., Marconi,M., Storm,J., et al. 2004,MNRAS, 344, 1097
Butler, D. 1975, AJ, 200, 68
Butler, D., Dickens, R.J., Epps, E. 1978, AJ, 225, 148
Carretta, E. & Gratton, R. 1997, A&AS, 121, 95
Clement, C. M., Muzzin, A., Dufton, Q., Ponnampalam, T., Wang,J., al. 2001, AJ, 122, 2587
Clementini, G., Gratton, R., Bragaglia, A., Carretta, E., at al. 2003, AJ, 125, 1309
Feast, M. 1992, in "Variable Stars and Galaxies", ed. Brian Warner (ASP: San Francisco), ASP Conf. Series 30, p. 143
Freeman, K. C., Rodgers, A. 1975, ApJ, 201, L71
Graff, D. S., Gould, A., Suntzeff, N. B., Schommer, R., & Hardy, E. 2000, ApJ, 540, 211
Gyuk, G., Dalal, N., & Griest, K. 2000, ApJ, 535, 90
Hardy, E., Alves, D., Graff, D., Suntzeff, N., Schommer, R. 2001, ApJSS, 277, 471
Jurcsik, J., 1998, ApJ, 506, 113
Kaluzny, J., Kubiak, M., M. Szymanski, M., Udalski, A., Krzeminski, W., et al. 1997, A&ASS, 122, 471
Kinman, T., Stryker, L., Hesser, J., Graham, J., Walker,A., at al. 1991, PASP, 103, 1279
Layden, A. 1994, AJ, 108, 1016
Liu, T. PASP 1991, 103, 205
Mayor, M., Meylan, G., Udry, S., Duquennoy, A., Andersen, J., at al. 1997, A&A, 114, 1087
Minniti, D., Borissova, J., Rejkuba, M., Alves, D., Cook, K.H., Freeman, K.C. 2003, Science, 301, 1508
Montegriffo, P., Ferraro, F., Origlia, L., Fusi Pecci, F. 1998, MNRAS, 297, 872
Olech, A., Kaluzny, J., Thompson, I.B., Schwarzenberg-Czerny, A. 2003, MNRAS, 345, 86O
Persson, S., Murphy, D., Krzeminski, W., Roth, M., Rieke, M. 1998, AJ, 116, 2475
Preston, G. 1959, ApJ, 130, 507

Rey, S., Lee, Y., Joo, J., Walker, A., Baird, S. 2000, AJ, 119, 1824
Sandage, A. 1981, ApJ, 244, L23
Smith, H. A. 1995, "The RR Lyrae Stars" (Cambridge Univ. Press)
Soszynski, I., Udalski, A., Szymanski, M., Kubiak, M., Pietrzynski, G., et al. 2003, Acta Astron., 53, 93
Stetson, P. 1994, PASP, 106, 250
van der Marel, R. P., Alves, D. R., Hardy, E., Suntzeff, N. B. 2002, AJ, 124, 2639
Walker, A. 1992, ApJ, 390, L81
Walker, A. 1998, astro-ph/9808336
Walker, A. 2003, astro-ph/0303011
Zebrun et al. 2001, Acta Astron., 51, 317
Zinn, R., & West, M.J. 1984, ApJS, 55, 45

This figure "0494f1.jpg" is available in "jpg" format from:

http://arXiv.org/ps/astro-ph/0405377v1